Sgluon pair production at the LHC with aMC@NLO
Validation figures

C. Degrande, B. Fuks, V. Hirschi,
J. Proudom & H.S. Shao

November 3, 2014

1 Simulation setup

Parton-level events have been simulated with the MadGraph5_aMC@NLO program [1], using the UFO module [2] generated by making use of FeynRules [3] and NloCT [4]. Hard scattering elements have been generated from the interactions embedded in the Lagrangian

$$\mathcal{L}_8 = \frac{1}{2} D_\mu \sigma_8 D^\mu \sigma_8 - \frac{1}{2} m_8^2 \sigma_8 \sigma_8 + \frac{\hat{g}_g}{\Lambda} \sigma_8 G_{\mu\nu} G^{\mu\nu} + \sum_{q=u,d} \Big[\sigma_8 \bar{q} \big(\hat{g}_q^L P_L + \hat{g}_q^R P_R \big) q + \text{h.c.} \Big] \ ,$$

as indicated in Ref. [5] where more information can be found. We recall that this Lagrangian describes the dynamics of a sgluon field σ_8 of mass m_8 that is allowed to decay into quarks and gluons via the $\hat{g}$ operators. We recall that the model is not suitable for single sgluon production at NLO. This requires to include, at tree-level, a *complete* basis of dimension-five operators to guarantee the cancellation, after renormalization, of all loop-induced ultraviolet divergences exhibiting a higher-dimensional Lorentz structure.

The numerical study presented in this document is based on of benchmark scenarios inspired by an R-symmetric supersymmetric setup where supersymmetry breaking induces non-minimal flavour violation in the squark sector [6]. The only non-vanishing coupling parameters are fixed to

$$\frac{\hat{g}_g}{\Lambda} = 1.5 \cdot 10^{-6}\ \text{GeV}^{-1} \ , \qquad (\hat{g}_u^{L,R})_{3i} = (\hat{g}_u^{L,R})_{i3} = 3 \cdot 10^{-3} \quad \forall i = 1,2,3 \ .$$

We consider two benchmark points for which the sgluon mass is fixed to $m_8 = 500$ GeV and 1000 GeV. For each scenario, we have generated 10^6 events at the leading order accuracy and the same number at the next-to-leading order one. The generated sampels are inclusive in the sgluon decays.

Sgluon decays have been achieved by using the MadSpin [7] package, and parton-level events generated in this way have then be showered and hadronized as implemented in the Pythia 8.2 program [8]. Hadronized events have then been processed with an anti-k_T algorithm with a radius parameter set to $R = 0.4$ [9], as implemented in the FastJet program [10].

From all the reconstructed jets, only those with a transverse-momentum $p_T > 20$ GeV and a pseudrapidity $|\eta| < 2.5$ have been retained. In our analysis, we have also only considered leptons with $p_T > 10$ GeV and $|\eta| < 2.5$. Moreover, we have removed all leptons lying at an angular distance $\Delta R < 0.4$ of any selected jet. All the differential distributions presented here have been generated with MadAnalysis 5 [11], the normalization being fixed to an integrated luminosity of 100 fb^{-1}. In each figure, we indicate both the leading-order and next-to-leading results, as well as their ratio called K-factor (which is differential here).

2 Global event variables

We present in Figure 1 the missing energy distribution (left) and the total transverse hadronic activity (right) that are calculated as

$$H_T = \sum_{\text{hadronic particles}} \big| \vec{p}_T \big| \qquad \text{and} \qquad \not{E}_T = \Big| - \sum_{\text{visible particles}} \vec{p}_T \Big| \ ,$$

where the sum are performed over all the event particles.

3 Zero lepton analysis

From the inclusively generated event sample, we select events which do not feature any final state electron or muon. We present in Figure 2 various distributions illustrating the properties of the two leading jets.

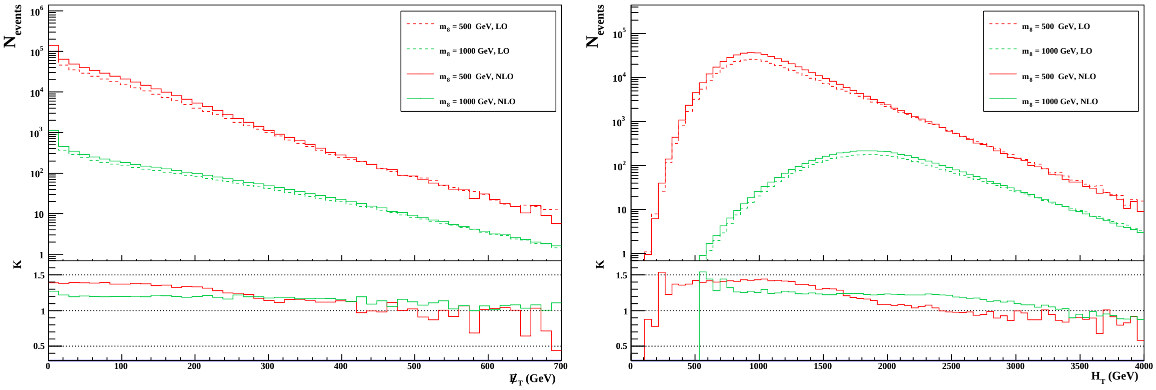

Figure 1: Global event variables: the missing transverse energy distribution (left) and the hadronic activity (right).

4 Single lepton analysis

From the inclusively generated event sample, we select events which feature exactly one final state electron or muon. We present in Figure 3 and Figure 4 various distributions illustrating the properties of the lepton and of the leading jets.

5 At-least-two-lepton analysis

From the inclusively generated event sample, we select events which feature at least two final state electrons or muons. We present in Figure 5, Figure 6 and Figure 7 various distributions illustrating the properties of the leptons and of the two leading jets.

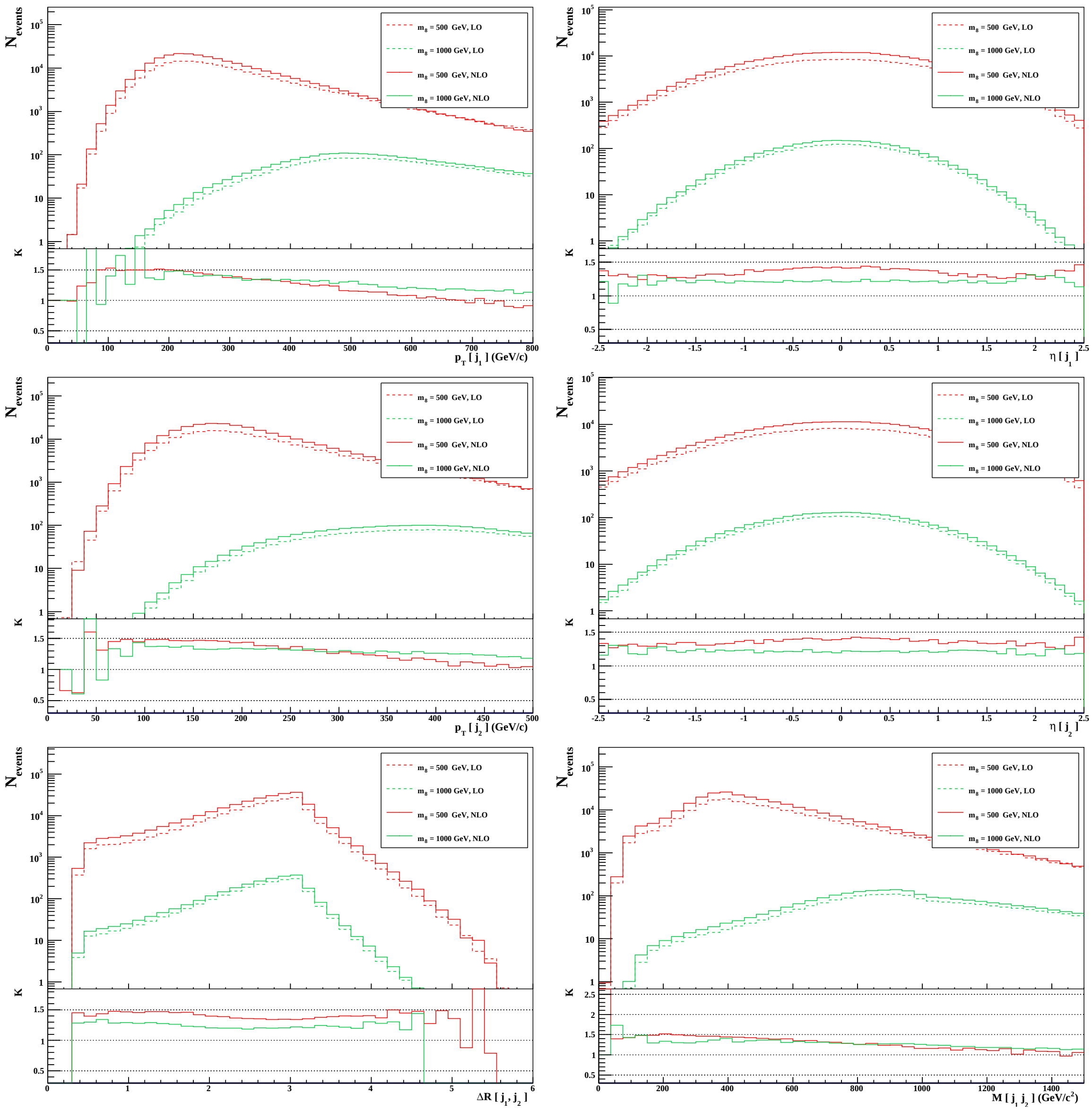

Figure 2: Zero lepton signal region: jet properties.

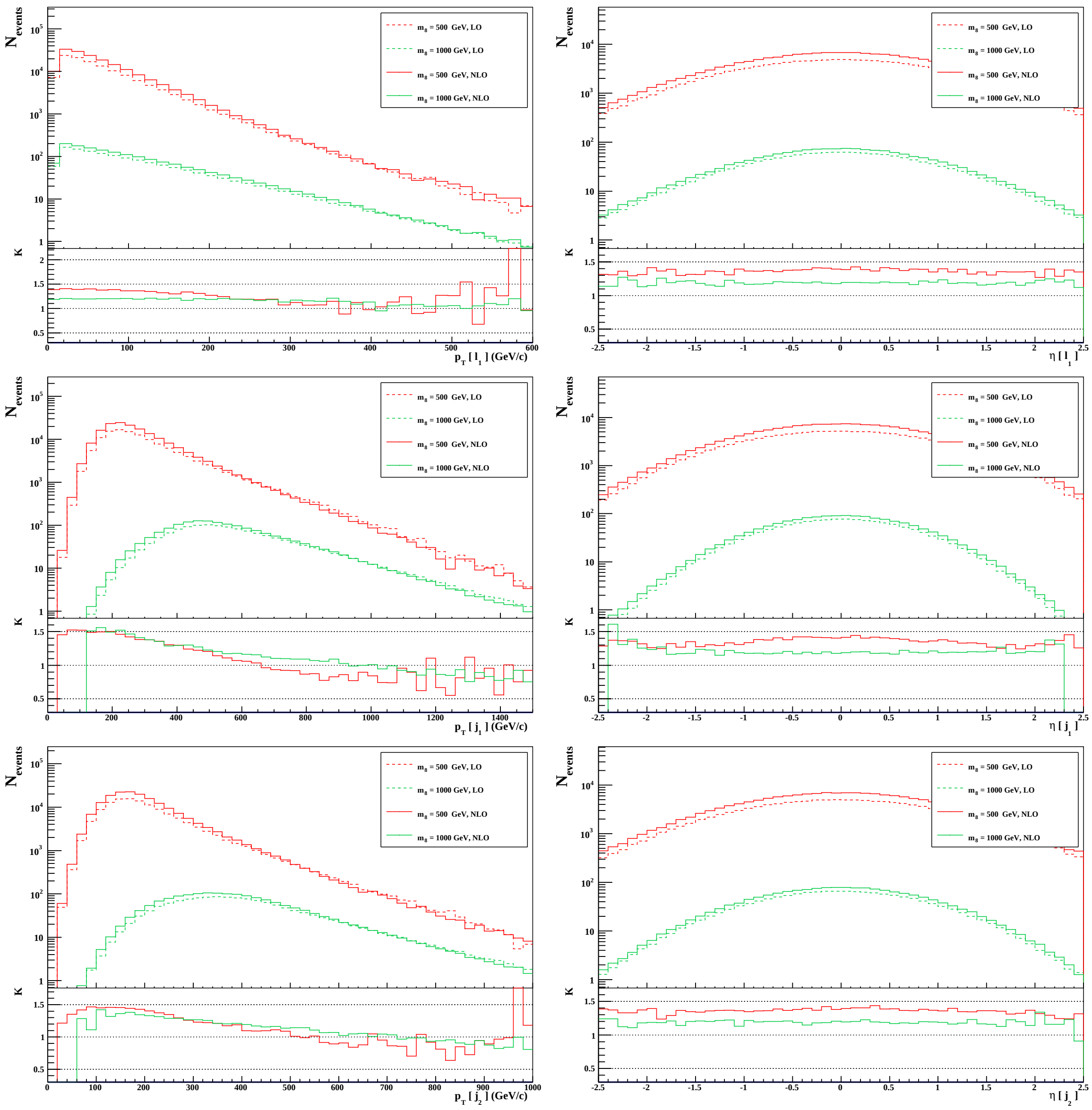

Figure 3: Single lepton signal region: lepton and jet properties.

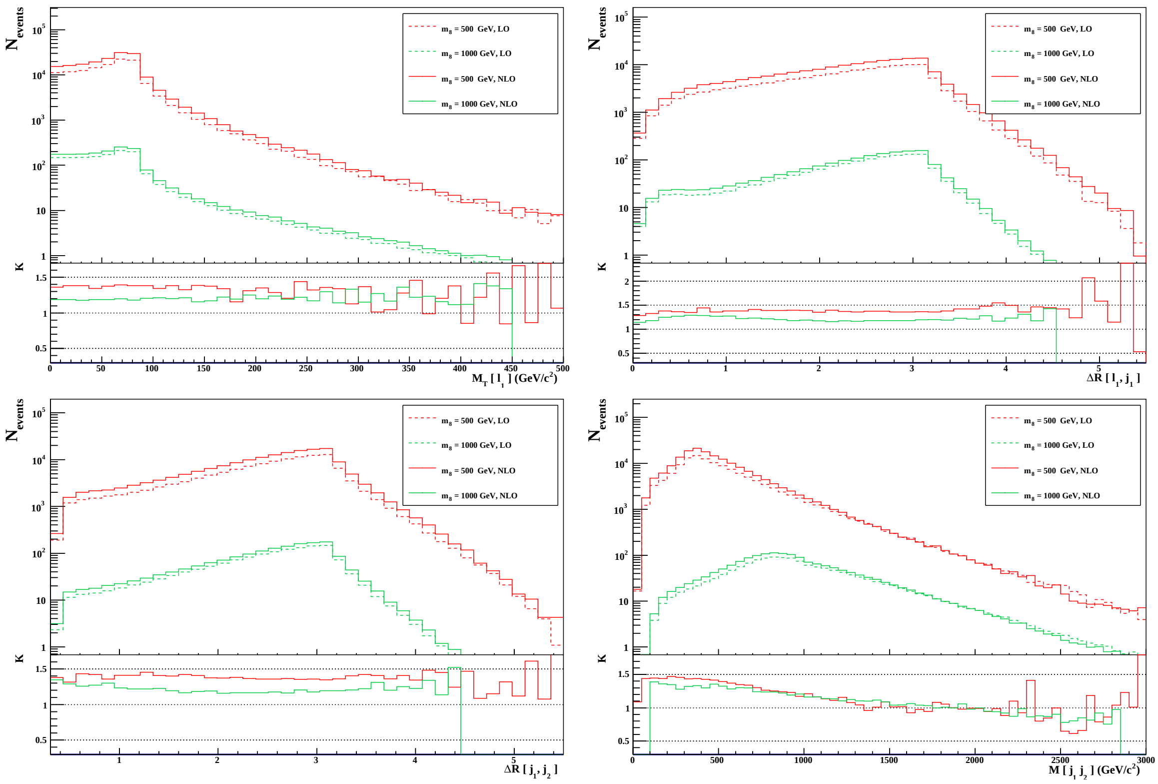

Figure 4: Single lepton signal region: lepton and jet properties (continued).

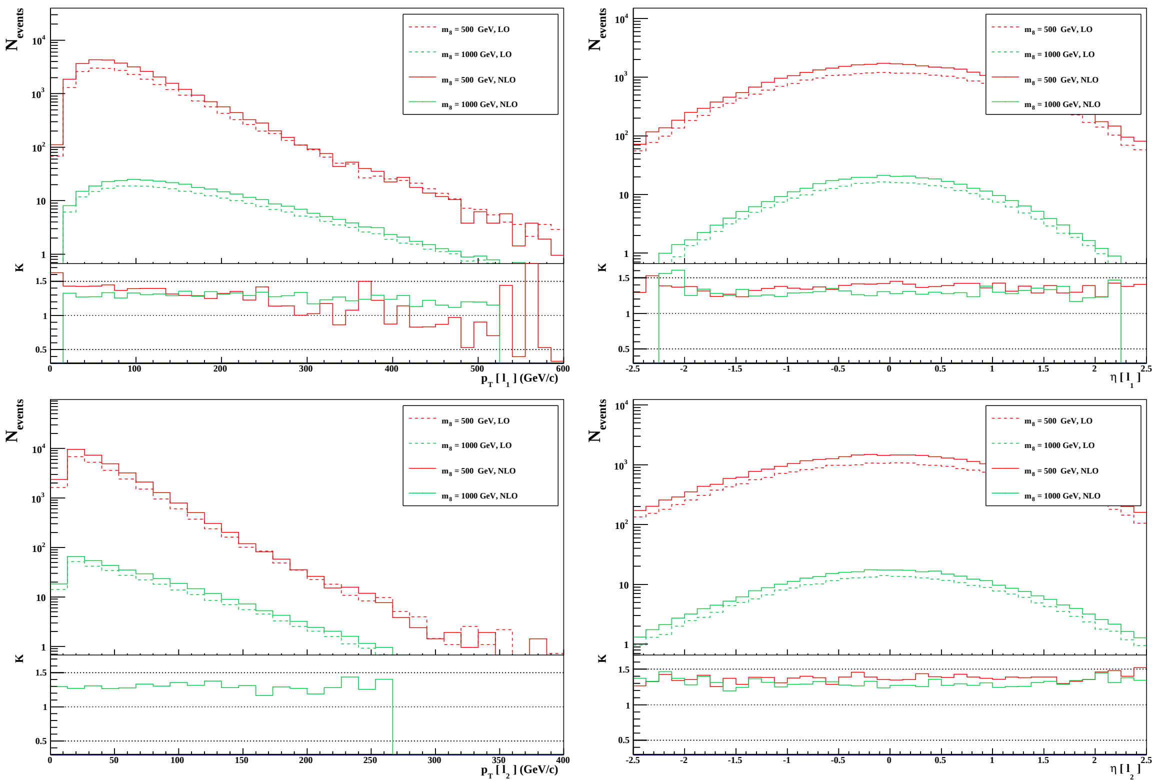

Figure 5: Multilepton signal region: lepton properties.

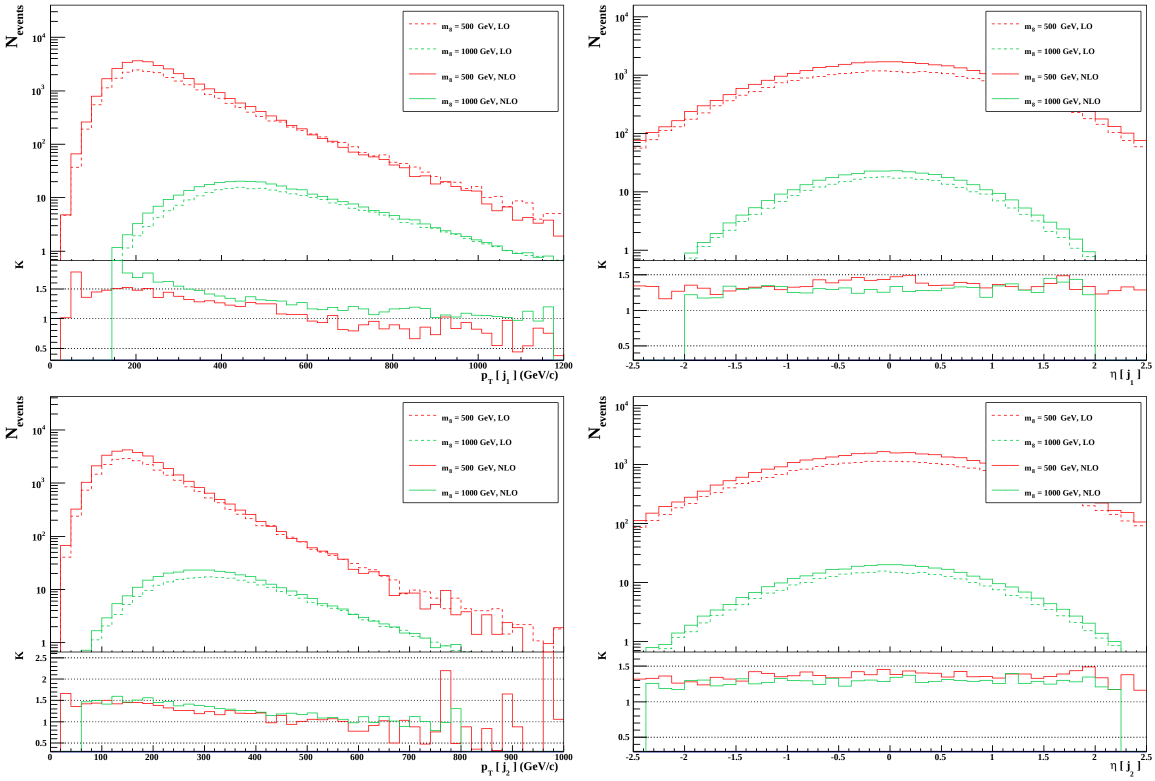

Figure 6: Multilepton signal region: jet properties.

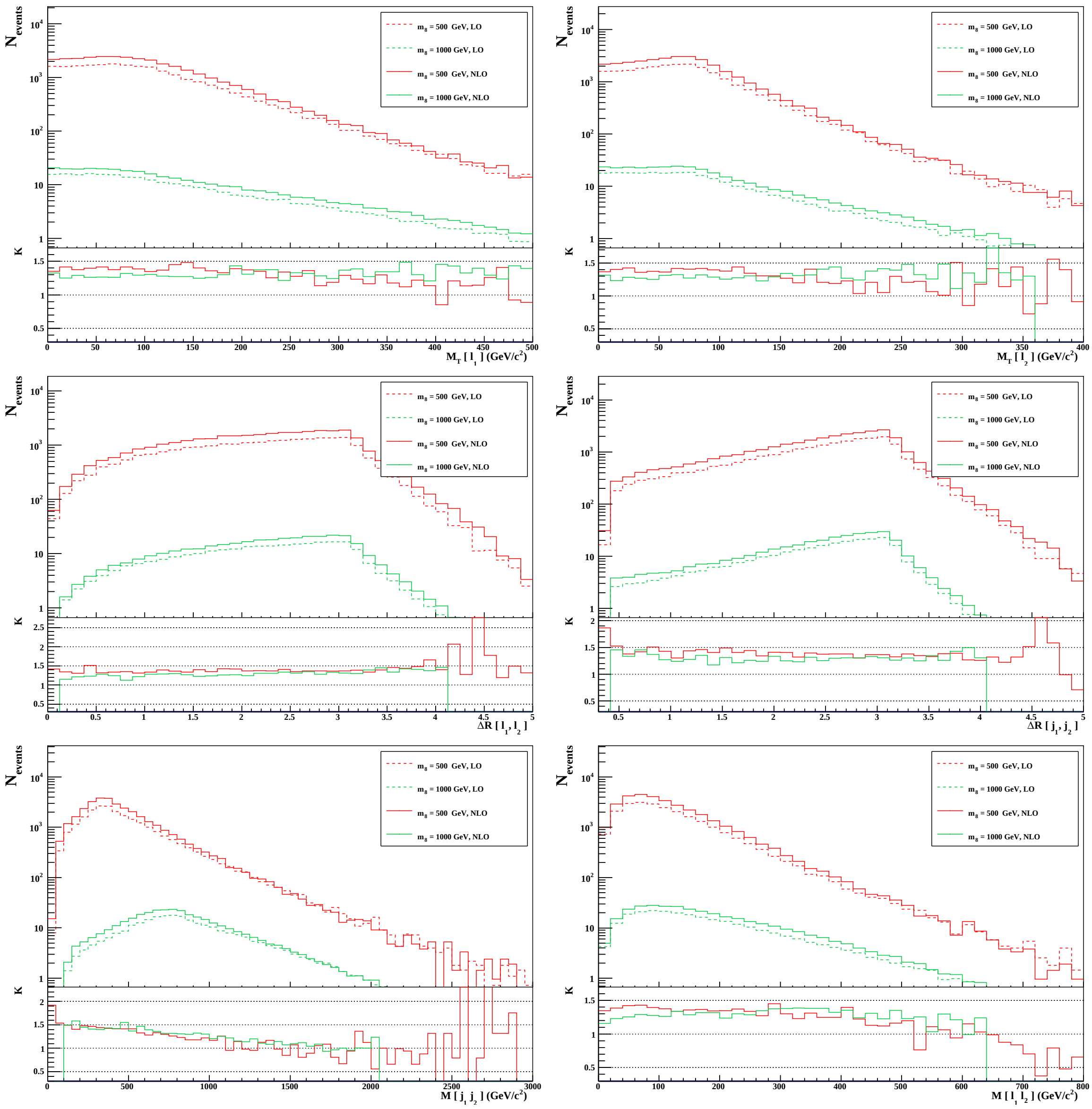

Figure 7: Multilepton signal region: jet and lepton properties (continued).

References

[1] J. Alwall, R. Frederix, S. Frixione, V. Hirschi, F. Maltoni, et al., *The automated computation of tree-level and next-to-leading order differential cross sections, and their matching to parton shower simulations*, *JHEP* **1407** (2014) 079, [arXiv:1405.0301].

[2] C. Degrande, C. Duhr, B. Fuks, D. Grellscheid, O. Mattelaer, et al., *UFO - The Universal FeynRules Output*, *Comput.Phys.Commun.* **183** (2012) 1201–1214, [arXiv:1108.2040].

[3] A. Alloul, N. D. Christensen, C. Degrande, C. Duhr, and B. Fuks, *FeynRules 2.0 - A complete toolbox for tree-level phenomenology*, *Comput.Phys.Commun.* **185** (2014) 2250–2300, [arXiv:1310.1921].

[4] C. Degrande, *Automatic evaluation of UV and R2 terms for beyond the Standard Model Lagrangians: a proof-of-principle*, arXiv:1406.3030.

[5] C. Degrande, B. Fuks, V. Hirschi, J. Proudom, and H.-S. Shao, *Automated next-to-leading order predictions for colored scalar production at the LHC*, to appear.

[6] S. Calvet, B. Fuks, P. Gris, and L. Valery, *Searching for sgluons in multitop events at a center-of-mass energy of 8 TeV*, *JHEP* **1304** (2013) 043, [arXiv:1212.3360].

[7] P. Artoisenet, R. Frederix, O. Mattelaer, and R. Rietkerk, *Automatic spin-entangled decays of heavy resonances in Monte Carlo simulations*, *JHEP* **1303** (2013) 015, [arXiv:1212.3460].

[8] T. Sjostrand, S. Mrenna, and P. Z. Skands, *A Brief Introduction to PYTHIA 8.1*, *Comput.Phys.Commun.* **178** (2008) 852–867, [arXiv:0710.3820].

[9] M. Cacciari, G. P. Salam, and G. Soyez, *The Anti-k(t) Jet Clustering Algorithm*, *JHEP* **0804** (2008) 063.

[10] M. Cacciari, G. P. Salam, and G. Soyez, *FastJet User Manual*, *Eur.Phys.J.* **C72** (2012) 1896.

[11] E. Conte, B. Fuks, and G. Serret, *MadAnalysis 5, A User-Friendly Framework for Collider Phenomenology*, *Comput.Phys.Commun.* **184** (2013) 222–256, [arXiv:1206.1599].